

## Thermomagnetic history effects in niobium and its implication for $H_{c1}$ in high $T_c$ superconductors

A K GROVER, P L PAULOSE, P CHADDAH\*  
and G RAVIKUMAR\*

Tata Institute of Fundamental Research, Homi Bhabha Road, Bombay 400005, India

\*Nuclear Physics Division, Bhabha Atomic Research Centre, Bombay 400085, India

MS received 30 March 1989

**Abstract.** The existence of a remanent magnetization ( $M_{rem}$ ) on switching off the field of a field cooled (FC) sample of a high  $T_c$  superconductor is often reported. It has recently been argued that  $M_{rem}$  should equal the difference in FC and zero field cooled (ZFC) magnetizations ( $M_{FC} - M_{ZFC}$ ) in hard superconductors and this has been demonstrated to hold in single crystals of YBCO at 4.2 K over a limited range of  $H$  values. We report the detailed magnetization measurements under various thermomagnetic histories (of which  $M_{rem}$  is one special case) on two specimens of Nb, which show different extents of flux trapping. We find that there are in general three regions in  $H$ ,  $T$  space, corresponding to  $M_{rem} + M_{ZFC} - M_{FC} = 0$ ,  $M_{rem} < (M_{FC} - M_{ZFC})$  and  $M_{rem} > (M_{FC} - M_{ZFC})$ . At any  $T$ , the equality holds for  $H < H_{c1}(T)$ , and for  $H \rightarrow H_{c2}$  ( $M_{FC} - M_{ZFC}$ ) asymptotically vanishes and there  $M_{rem} > (M_{FC} - M_{ZFC})$ . We show that there exists an intermediate region in all hard superconductors, where  $M_{rem} < (M_{FC} - M_{ZFC})$ . The range over which this situation persists, however, depends on the degree of irreversibility in a sample. We can explain qualitatively all the history dependent magnetization data in terms of the critical state model. We point out an inconsistency in an earlier analysis to determine  $H_{c1}(T)$  from such data in YBCO. We also propose a new criterion for putting limits on  $H_{c1}(T)$  in hard superconductors.

**Keywords.** Thermomagnetic history effects; Conventional type II superconductors; High temperature superconductors; Magnetization curves; Lower critical field.

**PACS Nos** 74·30; 74·60; 74·70

### 1. Introduction

The magnetization of a hard type II superconductor at a given temperature and magnetic field is known to depend on its thermomagnetic history. In the recent past, numerous workers have reported history dependent magnetization data on high  $T_c$  materials, which are also of type II variety. In spite of voluminous work, there are several basic aspects of these studies on which a consensus is yet to emerge (see, for instance, chapter titled 'Superconductivity–Glass phenomena' in Müller and Olsen (eds), 1988; Müller *et al* 1987; Malozemoff *et al* 1988a, b; Yeshurun and Malozemoff 1988; Fraser *et al* 1988; Ravi Kumar and Chaddah 1988; Grover *et al* 1988; Chaddah and Ravikumar 1989; Chaddah *et al* 1989; Rossel *et al* 1989). We feel that the divergence of views is partly due to an inadequate information in the literature relating to such issues in conventional type II superconductors (see, for instance, Schiedt *et al* 1988). We have therefore initiated a systematic study of thermomagnetic history and temporal effects in magnetization of conventional superconductors so as to compare their

behaviour with those in high  $T_c$  superconductors. For instance, the existence of a remanent magnetization ( $M_{\text{rem}}$ ) on switching off the field of a field cooled (FC) sample of a high  $T_c$  superconductor is often noted and its temperature dependence studied. Malozemoff *et al* (1988a) have argued that  $M_{\text{rem}}$  should equal the difference in FC and ZFC magnetizations at the same field and temperature and this equality is shown to hold in ceramic and single crystal specimens of  $\text{YBa}_2\text{Cu}_3\text{O}_7$  (YBCO) at 4.2 K up to 60 Oe. We have studied two samples of elemental niobium, a conventional type II superconductor with a  $T_c$  of about 9 K, which show different degree of flux trapping. We report in this paper the detailed magnetization measurements made on them under various thermomagnetic history cycles. We find similarities with the limited results for YBCO, and identify field and temperature regions where the equality,  $M_{\text{rem}} - M_{\text{FC}} = -M_{\text{ZFC}}$ , is valid. As for YBCO, we find the equality replaced first by an inequality  $<$  and later by  $>$ , as the temperature is raised at a constant field. Based on our extensive data, we identify three magnetic field regions in an isothermal magnetization hysteresis curve, and we relate these to a given applied field value ( $< H_{c1}(\text{O})$ ) falling in different field regions as the temperature is varied. We explain the history dependent magnetization curves to be consistent with the critical state model as applied to conventional type II and high  $T_c$  superconductors. We finally discuss the implications of our analysis for a new criterion for the determination of lower critical field  $H_{c1}$  in hard type II superconductors.

## 2. Experimental

### 2.1 Samples

Of the two Nb samples, one is 99.9% pure Nb powder obtained from Koch Light, UK and sieved through a 65 micron mesh, whereas the other is a piece with average length = 2.5 mm and average diameter = 2.6 mm, cut out of a niobium rod (purity 99.9%) obtained from Leico Industries, USA. The samples were used in as obtained condition, they were not subjected to any outgassing procedure. Nb is a hard type II superconductor because of absorbed oxygen and nitrogen, and the extent of irreversibility is known to decrease on outgassing (DeSorbo 1963; 1964; Finnemore *et al* 1966). There was interest in studying samples with different degree of flux trapping on field cooling. As will be evident from the results shown in the next section, the above two samples sufficed for the objective of the present investigations.

### 2.2 Magnetization measurements

DC magnetization measurements were performed employing Faraday method. The magnetic field was produced by an electromagnet and the field gradient was obtained using a pair of Lewis coils (Lewis 1971). The gradient field values used ranged between 3 to 11 Oe/cm. The power supply of the electromagnet is such that the steady field could be continuously ramped up and down between -50 Oe and 10 kOe at different speeds. The smallest step size in field variation was about 1.6 Oe. The applied field values were read using a Hall probe placed outside the cryostat. The Nb powder sample used had approximately the same mass as that of the piece cut from the Nb rod. The samples were mounted inside a gold plated copper bucket with ID = 4 mm and length 5 mm. The presence of Helium exchange gas ensured the rapid attainment

of thermal equilibrium between the sample and its surroundings. The temperatures were monitored by AuFe-chromel thermocouple stuck to the outer surface of the copper tubing surrounding the sample holder. The field gradient was switched on only while recording the pull at a fixed field value. The force was recorded about a minute after switching on the field gradient. The force value with the field gradient in the reversed direction was not recorded to avoid any possible complications due to hysteresis. The isothermal magnetization data were recorded at a nominal temperature of 5 K, where it was possible to ensure the stability to within  $\pm 0.2$  K over a few hours. The temperature dependence of magnetization in a fixed field value was recorded by ramping the heater current very slowly. The rate of increase in temperature was maintained in the range 30 to 50 mK/min.

As mentioned earlier, a major motivation of the present study is to understand history effects in hard type II superconductors. Isothermal magnetization measurements were made with the following sample histories:

- (i) Samples were cooled down to about 5 K in nominal zero field. These ZFC samples were then subjected to increasing fields up to a maximum of 5 kOe for Nb powder, and up to 3 kOe for Nb rod. This so called virgin magnetization is denoted by  $M_{ZFC}(H)$ . The field was reversed from the respective maximum values and the hysteresis in magnetization was recorded while reducing the field to zero. The  $M_{ZFC}(H)$  curves are shown in figures 1 and 2.
- (ii) Samples were cooled in different fixed field values from well above  $T_c$  to about 5 K. The magnetization of the field cooled specimen was recorded in each case and is referred to as  $M_{FC}(H)$ . Magnetization was then measured isothermally as a function of increasing field. This will be referred to as forward magnetization of a FC(H) sample. The field was reversed from 5 kOe (3 kOe) for the Nb powder (rod) specimen to obtain the hysteresis magnetization. Figure 1a shows such data in the powder sample for  $H = 200, 500$  and  $1000$  Oe, whereas figure 2a shows similar data in the rod for  $H = 200, 500, 1000$  and  $1700$  Oe.  $M_{FC}(H)$  values at 5 K for powder sample were also recorded at several other field values in the range 0 to 2 kOe. Figure 1d contains a plot of these data up to 300 Oe. At and above 500 Oe,  $M_{FC}(H)$  values are only marginally lower than the  $M_{ZFC}(H)$  values corresponding to the hysteresis cycle (i.e.; obtained on reversal of field from 5 kOe, see figure 1b).
- (iii) Powder and rod samples were cooled down to 5 K in the above mentioned respective fields. The field was then ramped down towards zero and magnetization measured along these reversed paths (see figures 1b, 1c and 2b). These will be referred to as reversed magnetization of a FC(H) sample. The remanent magnetization,  $M_{rem}(H)$  introduced in §1 is the magnetization corresponding to  $H = 0$  point on a given reverse magnetization curve.
- (iv) The virgin and hysteresis magnetization data on a ZFC Nb powder sample were recorded up to three other maximum field values, viz.,  $H_{max} = 75, 250$  and  $500$  Oe (see figure 1e). In the case of  $H_m = 75$  Oe, the forward (virgin and reverse magnetization (reversed data points not shown in figure 1e) lines coincide and there is no hysteresis, whereas for  $H_{max} = 250$  Oe, there is a tiny hysteresis. The hysteresis builds up rapidly as  $H_{max}$  increases towards 500 Oe.

Figure 3 shows the temperature dependences of  $M_{ZFC}(H)$ ,  $M_{FC}(H)$  and  $M_{rem}(H)$  in Nb powder, recorded during warm up from 4.7 K for  $H = 40, 75$  and  $300$  Oe. To record these data, the specimen was first cooled down to the lowest possible

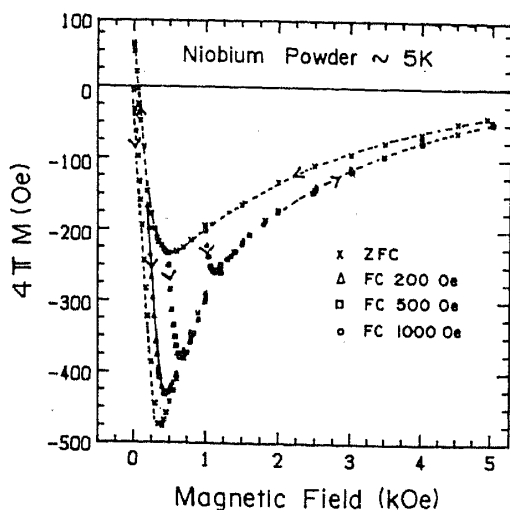


**Figure 1a.** Forward and hysteresis magnetization curves in the range 0 to 5 kOe at  $5 \pm 0.2$  K in Nb powder sample. The sample was cooled down from above its  $T_c$  to 5 K each time in nominal zero (ZFC), 200 Oe, 500 Oe and 1000 Oe respectively. The field was then increased up to 5 kOe before reversing down to zero value. The data points on reversal from 5 kOe have been shown only in ZFC case from clarity. For the rest of the cases, the data points overlap with the ZFC run. The dotted line passing through ZFC magnetization data points is a guide to the eye. It sketches out an envelope, within which the rest of FC magnetization curves are constrained to lie.

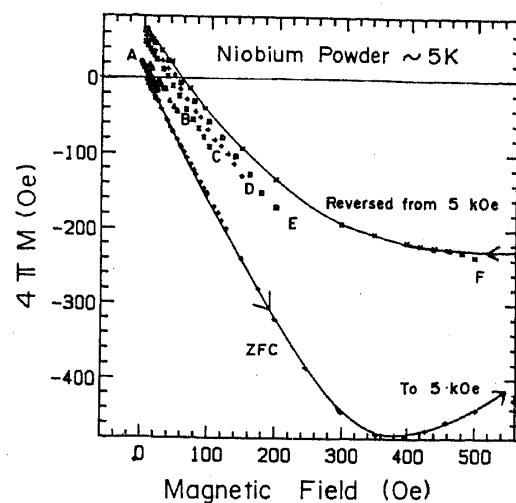


**Figure 1b.** Magnetization curves on reversal of field down to zero value from different field values in which Nb powder specimen is initially cooled down to  $5 \pm 0.2$  K each time. (A) FC in 20 Oe, (B) FC in 50 Oe, (C) FC in 100 Oe, (D) FC in 150 Oe, (E) FC in 200 Oe and (F) FC in 500 Oe. The solid line sketches out an envelope through ZFC data as explained in figure 1a. The reverse magnetization data points in the case F almost lie on this envelope.

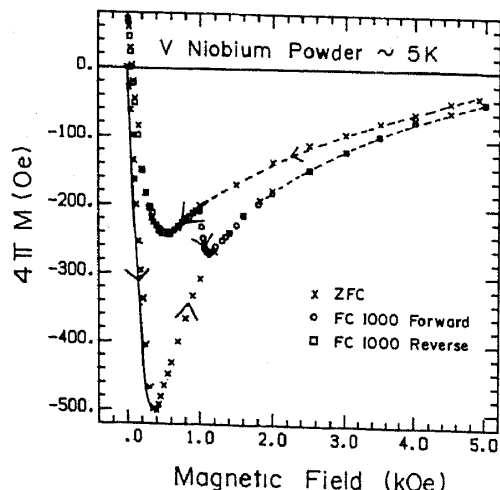


**Figure 1c.** Forward and reverse magnetization data obtained after cooling the Nb powder specimen down to  $5 \pm 0.2$  K in 1000 Oe. The figure also contains ZFC data to highlight the comparison between the two cases.

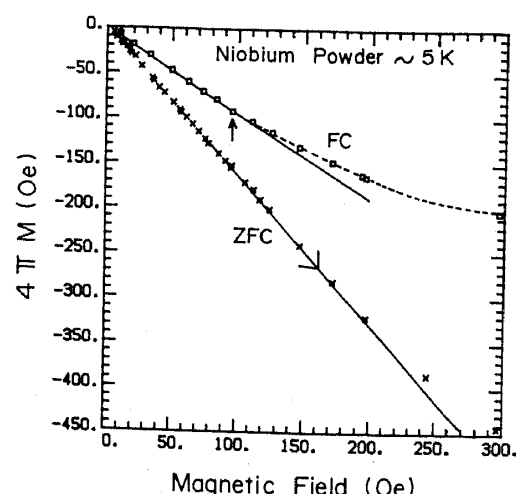


**Figure 1d.** A comparison of FC and ZFC magnetization curves in fields up to 300 Oe at 5 K in Nb powder. The arrow roughly marks the field value at which FC magnetization curve deviates from the initial linear behaviour.

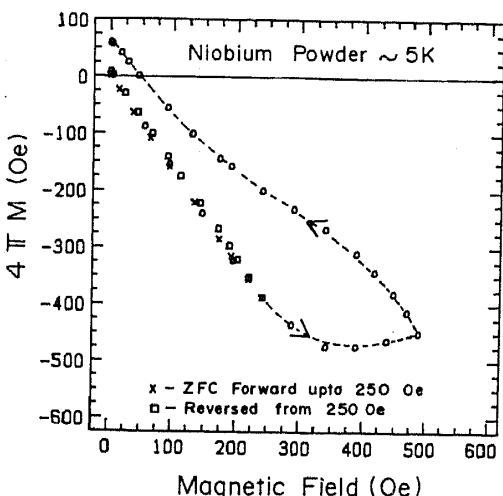


Figure 1e. Forward and hysteresis magnetization curves on reversal from  $H_{\max}$  of 250 Oe and 500 Oe at  $5 \pm 0.2$  K in a ZFC Nb powder specimen. In the case of reversal from  $H_{\max}$  of 75 Oe, the forward and hysteresis data points (not shown here) overlap.

temperature in nominal zero field. A given field value was then applied and magnetization measured ( $M_{ZFC}$ ) during warm up to temperatures above  $T_c$ . The sample was then cooled down to the lowest temperature in the same field and magnetization measured ( $M_{FC}$ ) during warm up cycle. After this, the sample was again cooled down to the lowest temperature in the same field. The field was then isothermally reduced to zero and the remanent magnetization ( $M_{rem}$ ) measured during warm up in nominal zero field. It may be remarked here that in the measurement of  $M_{rem}$ , the presence of a tiny field produced by the field gradient of about 6 Oe/cm on the finite sized sample was inevitable. The field cooled magnetization of Nb rod was nearly zero. Therefore, only the temperature dependences of  $M_{ZFC}$  and  $M_{rem}$  were recorded in this case. Figure 4 shows the plots for  $H = 200$  and 1000 Oe. The data in figures 3 and 4 have been normalized to the respective  $M_{ZFC}$  values at the lowest temperature.

### 3. Results

#### 3.1 Isothermal magnetization

The initial portion of the virgin ZFC magnetization curve at 5 K for Nb powder is shown on an expanded scale in figures 1b and 1d. Its initial slope value corresponds to  $-4\pi M/H$  of about 1.64. Equating this to  $1/(1 - N)$ , the average demagnetization factor  $N$  turns out to be 0.39. This may be compared with the theoretical value of 1/3 for perfectly spherical particles.

The virgin magnetization curve of Nb powder at 5 K peaks at about 400 Oe (figures 1a and 1b), and the magnetization decreases to < 10% of its value at turnover point at about 5 kOe. On reversing the field at 5 kOe, the magnetization hysteresis

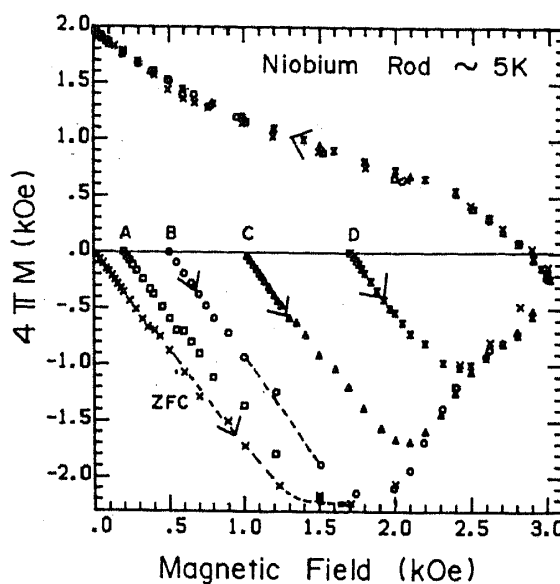


**Figure 2a.** Forward and hysteresis magnetization curves in the range 0 to 3 kOe at  $5 \pm 0.2$  K in Nb rod sample of average length = 2.5 mm and average diameter = 2.6 mm. The specimen was cooled down to 5 K each time in nominal zero, 200 Oe (A), 500 Oe (B), 1000 Oe (C) and 1700 Oe (D) respectively. As in figure 1a, the ZFC magnetization data points appear to sketch out an envelope within which the rest of the magnetization curves are constrained to lie.

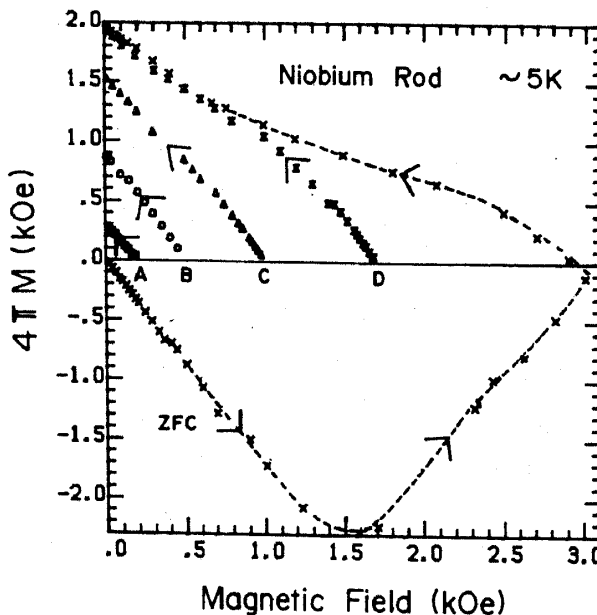


**Figure 2b.** Magnetization curves on reversal of field down to zero value from different field values in which Nb rod specimen is cooled down to  $5 \pm 0.2$  K each time. (A) FC in 200 Oe, (B) FC in 500 Oe, (C) FC in 1000 Oe and (D) FC in 1700 Oe. The dotted line through the ZFC magnetization data points is a guide to the eye.

curve continues to be diamagnetic. The hysteretic curve turns over at around 500 Oe and below about 60 Oe the magnetization moves towards positive values. The irreversibility in magnetization on reducing the field and the existence of a finite positive moment on the reverse hysteresis cycle confirms the hard type II nature of the superconducting sample. The ZFC Nb rod sample shows an order of magnitude,

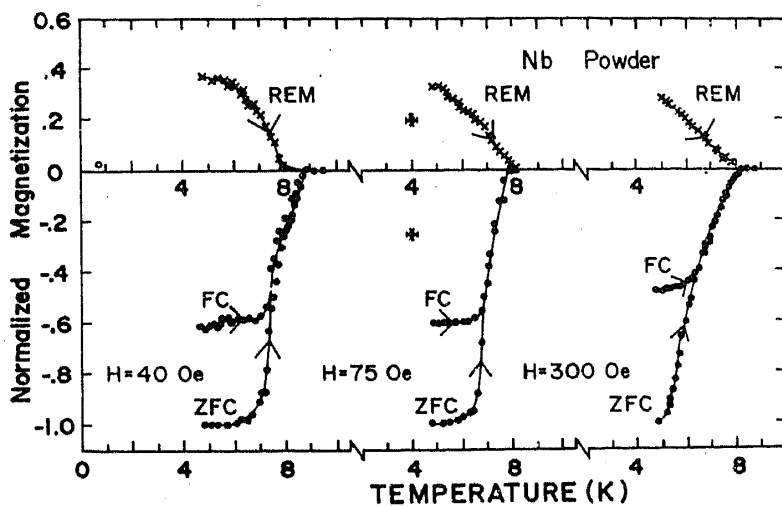


Figure 3. Temperature dependence of normalized values of  $M_{ZFC}$ ,  $M_{FC}$  and  $M_{rem}$  in Nb powder corresponding to three different field values, viz,  $H = 40$  Oe, 75 Oe and 300 Oe respectively. The arrows indicate the direction in which the temperature was varied. The solid lines have been drawn through the data points only to guide the eye.

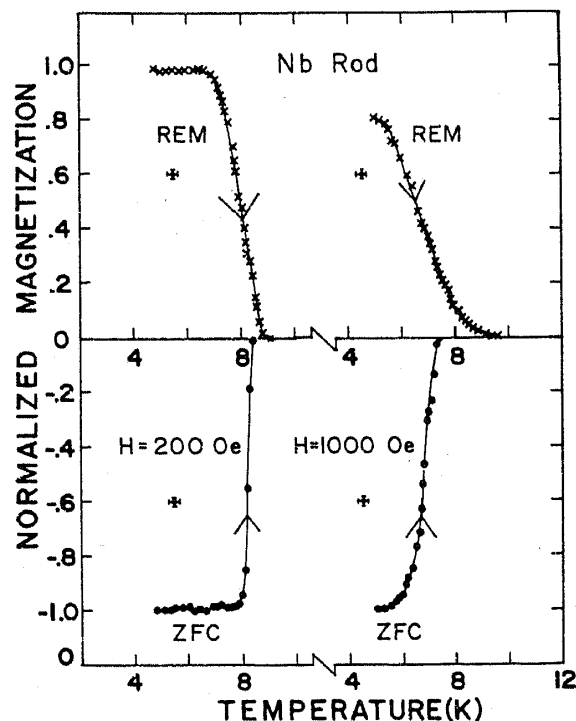


Figure 4. Temperature dependences of normalized values of  $M_{ZFC}$  and  $M_{rem}$  corresponding to  $H = 200$  Oe and 1000 Oe in Nb rod sample.  $M_{FC}$  value at the lowest temperature was nearly zero, therefore, its temperature dependence was not recorded. The arrows indicate the direction in which the temperature was varied. As in figure 3, the solid lines are drawn only to guide the eye.

larger irreversibility (cf. figures 1a and 2a) and the hysteresis magnetization is positive almost throughout the reverse cycle. Its virgin magnetization at 5 K turns over at about 1.7 kOe, and as compared to Nb powder, the peak magnetization is about five times larger.

The Nb powder sample shows a partial flux trapping at low field values (figure 1d), whereas the Nb rod sample shows almost complete flux trapping on field cooling (figure 2a). However, the isothermal magnetization data recorded after field cooling display similar physical phenomena in both the samples. The salient features of these are detailed as follows:

- (i) The initial slope value of the forward magnetization of any given FC( $H$ ) state (figures 1a and 2a) appears to be the same as that of the respective virgin ZFC curves.
- (ii) A forward magnetization FC( $H$ ) curve merges with the virgin ZFC curve (figures 1a and 2a). This merger occurs at some field value  $H_m$ , which is different for different forward magnetization curves in each sample. The field interval,  $H_m - H$ , required for this merger decreases as  $H$  increases. The merger and the consequent loss of thermomagnetic memory, continues even during the hysteresis cycle on reversing the field from  $H_{\max}$ .
- (iii) The reverse magnetization of a FC( $H$ ) sample is linear for small  $H$  and the slope appears to be the same as that of the initial linear portion of the ZFC curve. The equality of two slope values between 0 and  $H$  imply the relation,  $M_{\text{ZFC}}(H) = M_{\text{FC}}(H) - M_{\text{rem}}(H)$ . In the case of Nb powder at 5 K, this situation appears to hold below about 100 Oe (figure 1b), whereas for Nb rod it extends up to about 500 Oe (figure 2b). Above these limiting values, the slope of the reverse magnetization decreases. As  $H$  is increased further, the reverse magnetization curve becomes non-linear, however, it appears to be constrained to lie within the envelope provided by the ZFC hysteresis curve. This is best illustrated by the curve F in figure 1b and the curve labelled FC 1000 reverse in figure 1c for the Nb powder, and the curve D in figure 2b for the Nb rod. Since  $M_{\text{rem}}$  is the intercept of the reverse magnetization curve with the  $H = 0$  line, we note that we have results for  $M_{\text{rem}}(H)$ ,  $M_{\text{FC}}(H)$  and  $M_{\text{ZFC}}(H)$  over the whole range of  $H$  values. In the next section, we shall identify regions in isothermal magnetization data, for which  $(M_{\text{rem}}(H) - M_{\text{FC}}(H))$  is equal to, less than, and greater than  $-M_{\text{ZFC}}(H)$ .
- (iv) Figure 1d shows a comparison of  $M_{\text{ZFC}}(H)$  and  $M_{\text{FC}}(H)$  data as the same temperature in Nb powder. The ratio of the initial slope values in the two cases imply that about 42% of magnetic flux remains trapped on field cooling Nb powder specimen. The field value of about 100 Oe, at which the  $M_{\text{FC}}(H)$  curve appears to deviate from linearity is not different from the field limit up to which the equality,  $M_{\text{ZFC}} - M_{\text{FC}} + M_{\text{rem}} = 0$  holds at the same temperature. Further, it may be pointed out that no measurable hysteresis in magnetization was observed on reversing the field from  $H_{\max}$  of 75 Oe on a ZFC specimen (see figure 1e). Such a comparison of  $M_{\text{FC}}$  and  $M_{\text{ZFC}}$  data in Nb rod cannot be carried out on the basis of our data, since  $M_{\text{FC}}(H)$  is zero within the reliability of the method adopted by us to measure magnetization of superconductors.

### 3.2 Temperature dependent magnetization

Figures 3 and 4 show the temperature dependences of normalized values of  $M_{\text{ZFC}}(H)$ ,

$M_{FC}(H)$  and  $M_{rem}(H)$  for a few different values of  $H$  in Nb powder and Nb rod. As stated above, for low fields, the equality  $M_{rem}(H) = (M_{FC}(H) - M_{ZFC}(H))$  is satisfied at the lowest temperature. This is illustrated for  $H = 40$  Oe and  $H = 200$  Oe data in figures 3 and 4 respectively. At high fields,  $M_{rem}(H) < (M_{FC}(H) - M_{ZFC}(H))$  even at the lowest temperature, as is evident from  $H = 300$  and 1000 Oe data in figures 3 and 4 respectively. However, as the temperature is raised, we move into the regime,  $M_{rem} < (M_{FC} - M_{ZFC})$ , even for those fields for which the equality is satisfied at the lowest temperature. As temperature rises further, the inequality gets reversed, such that  $M_{rem} > (M_{FC} - M_{ZFC})$ . In fact, in Nb powder we observe that  $M_{FC}$  and  $M_{ZFC}$  data points overlap (see all the three data sets in figure 3) within the accuracy limits over some range close to  $T_c$ . The width of the overlap region is larger for higher field and, in this temperature region the inequality  $M_{rem} > (M_{FC} - M_{ZFC})$  trivially holds.

In Nb rod,  $M_{FC}(H, T) = 0$ . But, the transition corresponding to  $M_{rem}$  being  $>$  to  $< (M_{FC} - M_{ZFC})$  can be clearly observed in both the data sets of figure 4. The temperature variations of  $M_{rem}$  and  $M_{ZFC}$  in  $H = 1000$  Oe in Nb rod focus attention onto another interesting point. There is an appreciable temperature region just below  $T_c$ , where  $M_{ZFC} = M_{FC} = 0$ , but  $M_{rem} \neq 0$ . This is due to the fact that the quantity  $M_{rem}$  is measured in zero external field, whereas both  $M_{ZFC}$  and  $M_{FC}$  are measured in a given external field. Therefore, in the temperature region, where a given external field  $H$  is greater than the  $H_{c2}(T)$  value of the specimen, both  $M_{ZFC}(H)$  and  $M_{FC}(H)$  will be identically zero. However,  $M_{rem}$ , obtained after switching off a given field  $H$  at a given  $T (< T_c)$ , survives on warming up the specimen up to its  $T_c$  value.

The temperature dependent magnetization data in Nb samples thus show three  $(H, T)$  regions corresponding to  $M_{rem}$  being equal to or  $<$  or  $> (M_{FC} - M_{ZFC})$ . In the next section, we shall compare these with similar observations (Malozemoff *et al* 1988) in high  $T_c$  YBCO specimens, and discuss its consequences in the light of an understanding of the underlying physics.

#### 4. Discussion

We shall now present an exposition of the physical phenomena underlying our data using an extension of the critical state model due to Bean (1962, 1964). The basic premises used are

1. All isothermal changes of magnetic field cause changes in magnetization that are driven by changes in the thermodynamic magnetization as well as by shielding currents. The latter effect is specific to hard type II superconductors which have a finite  $J_c$ . It was first invoked by Bean (1962), and results in the virgin ZFC magnetization being larger in magnitude than the thermodynamic magnetization at any field greater than  $H_{c1}$ .
2. When a sample is cooled below  $T_c$  in a constant magnetic field, the sample magnetization can change only because of changes in the thermodynamic magnetization. The full thermodynamic magnetization may not be seen as trapping by pinning centres in a hard type II superconductor may not allow expulsion of flux. The field gradients in a FC sample occur over a length scale of the penetration depth. There are no macroscopic field gradients and thus no shielding currents in contrast to a sample which has been brought to the same field value after isothermal field changes.

#### 4.1 Model for isothermal magnetization

Bean's critical state model describes the isothermal magnetization of a ZFC sample. Assuming that  $H_{c1}$  is small and one can ignore the thermodynamic magnetization, the field profile inside a superconducting slab is governed by,

$$\frac{dB}{dx} = -(4\pi/10)J_c(B_z(x)). \quad (1)$$

The field profiles ( $B(x)$ ), for increasing values of applied field, are shown schematically in figure 5a. The figure incorporates the decrease of  $J_c$  with increasing field, and this is depicted by the fact that the magnitude of the field gradient is smaller at larger fields. There is an applied field  $H_I$  at which the flux penetrates the entire sample, and the virgin ZFC magnetization peaks at a field  $H < H_I$ . This follows trivially from the fact that the magnetization  $M$  is given as,

$$\begin{aligned} 4\pi M &= (1/D) \int_{-D/2}^{D/2} (B(x) - H_{app.}) dx \\ &= (2/D) \int_0^{D/2} x J_c(x) dx \end{aligned} \quad (2)$$

where  $J_c(x)$  decreases throughout the sample as the applied field is raised beyond  $H_I$ . While the description being given here is for a sample geometry of an infinite slab with  $N = 0$ , the basic results would remain unchanged for arbitrary  $N$ .

In figure 5b we consider a sample cooled in a low applied field  $H_1 < H_I$ . We assume that the flux is completely trapped on field cooling, as for our Nb rod sample, and this is depicted by a flat profile for  $B(x)$  at  $H_1$ . As the field is increased isothermally, the field profile is first modified only near the surface region. At a higher applied field  $H_3$ , which must be greater than  $H_I$ , the field profile is modified throughout the sample and is the same as that for a ZFC sample at  $H_3$ . The FC( $H_1$ ) forward curve thus merges with the ZFC curve at  $H_m(H_1) = H_3$ . While the peak in FC( $H_1$ ) forward curve must occur at  $H_{pk}(H_1) < H_3$ , it can also be argued from eq. (2) that  $H_{pk}(H_1) < H_{pk}(H_2)$  for  $H_1 < H_2$ .

To consider how  $H_m(H)$  varies with  $H$ , we show schematically in figure 5c, the field profiles corresponding to the forward magnetization of FC( $H_4$ ) sample. The field profiles have smaller gradient (in comparison to figure 5b) as  $J_c$  is smaller at these higher fields. The field profile is now modified throughout the sample at  $H_m(H_4) = H_7$ , at which field the FC( $H_4$ ) forward magnetization merges with the ZFC magnetization. We have depicted schematically in figures 5b and 5c that  $(H_m(H) - H)$  decreases with increasing  $H$ . This is a consequence only of  $J_c(H)$  decreasing with increasing  $H$ , and is exactly what is observed in both the rod and powder samples. While the powder sample does not show the complete flux trapping assumed in the above description, the physics of how to understand an isothermal variation of magnetization appears unchanged. The flat profile pinned at applied field  $H$  assumed on field cooling is probably not valid in Nb powder, but the evolution of the field profile with varying magnetic field is.

We now consider the reverse curve for a FC( $H$ ) sample and again assume complete flux trapping on field cooling. We depict schematically in figure 5d the field profiles as the applied field is decreased from  $H_4$ . For a small decrease in field, the profile is modified only in the surface region. The profile is modified throughout the sample

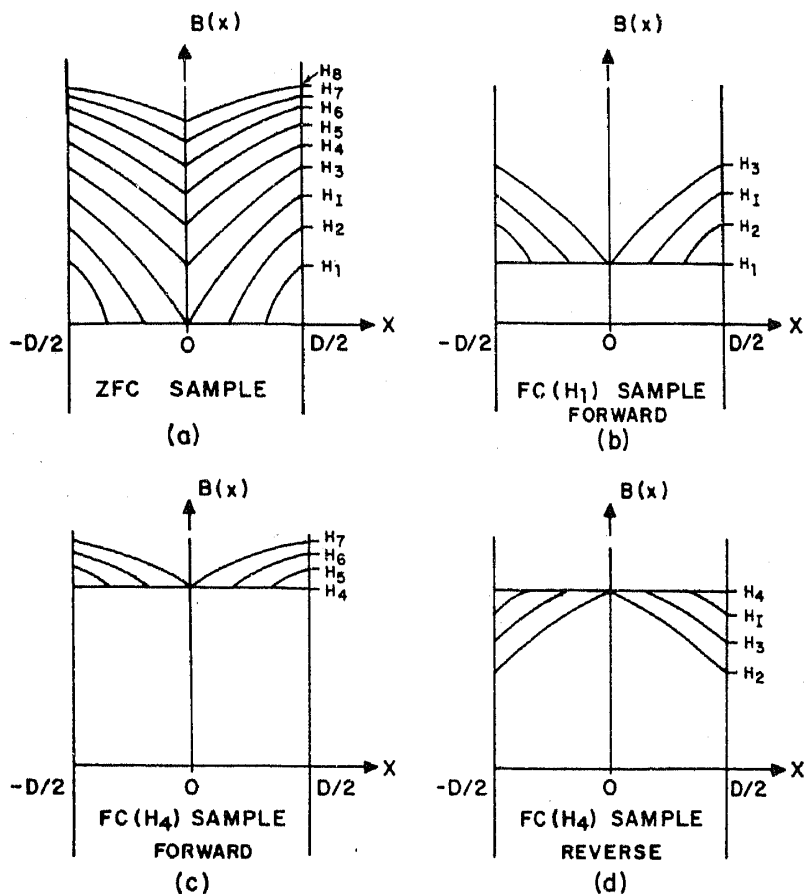


**Figure 5.** Schematic field profiles  $B(x)$  in a sample in the form of an infinite slab of thickness  $D$ , with the applied field along the sample surface.  $H_{c1}$  is ignored as very small and  $J_c(B)$  is assumed to decay with increasing field. (a) A ZFC sample as the external field is increased from  $H_1$  to  $H_8$ . Complete flux penetration occurs at  $H_1$ . (b) to (d). Field cooled samples with complete flux trapping. (b) depicts a  $FC(H_1)$  sample subjected to increasing field, while (c) depicts a  $FC(H_4)$  sample subjected to increasing field. In (d) the field profiles are shown for a  $FC(H_4)$  sample subjected to decreasing field.

only when the field is lowered to  $H_2$ , and the reverse  $FC(H_4)$  curve then merges with the reverse hysteresis curve of the ZFC sample. This merger will occur at positive fields for a  $FC(H)$  sample only if  $H > H_1$ . This is consistent with our results on the Nb (figure 2b) rod sample.

The behaviour of the powder sample on the reverse  $FC(H)$  curves cannot be fully explained in the above picture because of the partial flux trapping on field cooling and the smallness of  $H_1$  in Nb powder. Both these features do not allow us to neglect  $H_{c1}$ . We shall incorporate  $H_{c1}$ , though only in the isothermal behaviour, to explain another feature of the data in Nb rod and powder samples in the following discussion.

#### 4.2 Comparison of $M_{ZFC}$ , $M_{FC}$ and $M_{rem}$

Malozemoff *et al* (1988a) have experimentally found that in a variety of YBCO samples,

$$M_{rem}(H) = M_{FC}(H) - M_{ZFC}(H) \quad (3)$$

at 4.2 K. This relation is found to hold over the range of fields investigated (up to

60 Oe), and in samples with varying degree of flux trapping on field cooling. While their data show that relation (3) does not hold at arbitrary temperatures, we concentrate presently on the justification they offer for the validity of relation (3). Their basic assumption is that flux is completely excluded in a ZFC sample, i.e.,  $4\pi M_{ZFC}(H) = -H/(1-N)$ . This relation strictly holds for  $H < H_{c1}(1-N)$ , which thus defines the field region over which (3) can be valid. They also state, as an added assumption, that no flux is expelled from a FC( $H$ ) sample as the field is isothermally reduced to zero.

We shall now consider the case when  $H > H_{c1}(1-N)$ . As earlier, we shall assume complete flux trapping on field cooling, i.e.,  $M_{FC} = 0$  and also put  $N = 0$ . Above  $H > H_{c1}$ , we have to invoke shielding effects. We show in figure 6a the schematic field profiles in the ZFC case for  $H = H_1$ , where  $H_{c1} < H_1 < H_{c1} + H_I$ , and for  $H = H_6 (> H_I + H_{c1})$ . We note that a finite  $H_{c1}$  adds to the magnitude of  $M_{ZFC}(H_1)$ , but does not affect the magnitude of  $M_{ZFC}(H_6)$ . In figure 6b we show the flux profile for FC( $H_1$ ) as the field is reduced to zero. The field in the surface region is zero and

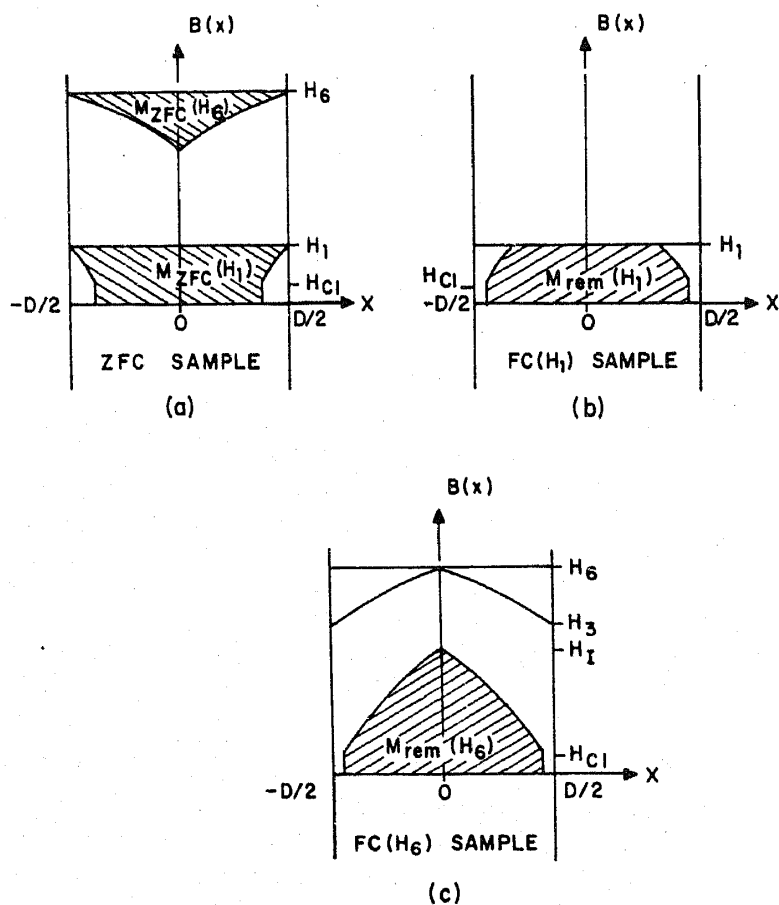


Figure 6. Schematic field profiles are shown as in figure 5, but for a non-zero value of  $H_{c1}$ . (a) depicts a ZFC sample subject to increasing field. The profiles are shown for external field values  $H_1$  and  $H_6$ .  $-4\pi M$  is the difference between the applied field and  $B(x)$ , as integrated over the sample. The values of  $M_{ZFC}(H_1)$  and  $M_{ZFC}(H_6)$  are thus proportional to the corresponding shaded areas. (b) depicts a FC( $H_1$ ) sample after the field is reduced to zero.  $4\pi M_{rem}(H_1)$  is just the total flux in the sample, and  $M_{rem}(H_1)$  is thus proportional to the shaded area. (c) depicts a FC( $H_6$ ) sample as the field is reduced to zero, and  $M_{rem}(H_6)$  is proportional to the shaded area.

then builds up suddenly to  $H_{c1}$ . In figure 6 we have implicitly assumed that the flux can be expelled during the reverse isothermal change, even though it is not expelled on field cooling. (However this assumption is not crucial to the following references). The value of  $M_{\text{rem}}(H_1)$  is proportional to the shaded area in figure 6b, and is clearly less than  $M_{\text{ZFC}}(H_1)$ , which is the shaded area in figure 6a. We thus find that the equality of Malozemoff *et al* (1988a) will be replaced by,

$$\left| M_{\text{rem}}(H) - M_{\text{FC}}(H) \right| < \left| M_{\text{ZFC}}(H) \right|. \quad (4)$$

The field at which this inequality will be seen provides an upper bound on  $H_{c1}$ .

In figure 6c we consider the flux profile for  $M_{\text{FC}}(H_6)$  as  $H$  is reduced to zero. The value of  $M_{\text{rem}}(H)$  is seen to be larger than  $M_{\text{ZFC}}(H_6)$ . This is because we have assumed  $J_c$  to be much lower at fields around  $H_6$  than at fields between 0 and  $H_1$ . We thus find that at large fields where  $J_c$  decays sharply with  $H$ , equality of Malozemoff *et al* gets replaced by the inequality,

$$\left| M_{\text{rem}}(H) - M_{\text{FC}}(H) \right| > \left| M_{\text{ZFC}}(H) \right|. \quad (5)$$

It is apparent from the schematic flux profiles shown that this occurs for  $H > H_1 + H_{c1}$ .

We have argued above that at any given temperature we must go through regions satisfying eqs (3), (4) and (5) as the applied field is increased. The arguments above have been presented for complete flux trapping as seen in our Nb rod sample. Partial flux trapping requires similar but more detailed arguments, and would yield a similar behaviour as the field is increased. As shown in figure 7, we clearly see the three regions for the Nb powder sample at 5 K. In figure 7, we have given a plot of the ratio  $(-M_{\text{ZFC}})/(M_{\text{rem}} - M_{\text{FC}})$  versus  $H$ . The horizontal line corresponds to eq. (3) whereas the data points above and below this line satisfy eqs (4) and (5) respectively.

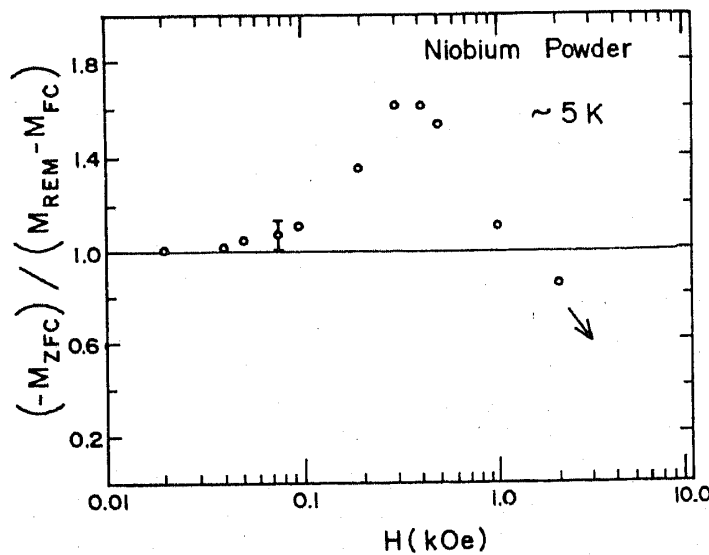


Figure 7. Field dependence of the ratio  $(-M_{\text{ZFC}})/(M_{\text{rem}} - M_{\text{FC}})$  in Nb powder at 5 K. A typical error bar has been indicated in the figure. The horizontal line corresponds to the equality,  $M_{\text{rem}} - M_{\text{FC}} + M_{\text{ZFC}} = 0$ .

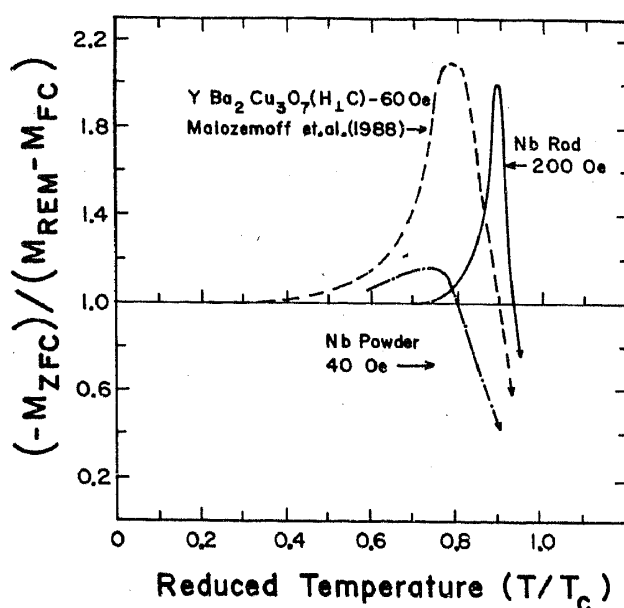


Figure 8. Temperature dependences of the ratio  $(-M_{ZFC})/(M_{rem} - M_{FC})$  in the specimens of Nb powder, Nb rod and single crystal ( $H \perp c$ ) of high  $T_c$   $YBa_2Cu_3O_7$  at the field values indicated in the figure.

For the rod sample (see figure 2b) the equality appears to hold at  $H = 500$  Oe, it is replaced by relation (4) at 1000 Oe, and relation (5) holds for  $H$  larger than 2000 Oe.

The three regions are encountered as the applied magnetic field is increased to  $H_{c1}$  and then to  $H_{c1} + H_I$ . Both  $H_{c1}$  and  $H_I$  (which varies with  $J_c(H)$ ) decrease as the temperature is increased. We thus expect to go through different regions as the temperature is varied for a fixed applied field. The experimental results in Nb powder and rod sample relating to this aspect have already been described in detail. Figure 8 shows the plots of the ratio  $(-M_{ZFC})/(M_{rem} - M_{FC})$  versus reduced temperature ( $T/T_c$ ) in Nb powder ( $H = 40$  Oe), Nb rod ( $H = 200$  Oe) and single crystal ( $H = 60$  Oe,  $\perp c$ ) of  $YBa_2Cu_3O_7$ . The curves for the first two samples correspond to smooth lines drawn through the data shown in figures 3 and 4, whereas the curve for high  $T_c$  specimen has been deduced from figure 2 of Malozemoff *et al* (1988a). The transitions through the three different regions are clearly apparent in all the three curves of figure 8. It is interesting to note the similarity in the behaviour of a conventional type II and a high  $T_c$  superconductor.

#### 4.3 Determination of $H_{c1}$

Bean (1962) had suggested that the field at which flux first penetrates a ZFC sample, to an experimentally measurable extent, would be dictated not only by  $H_{c1}$  but also by the size and  $J_c$  of the sample. The variation with size was demonstrated immediately (Hauser 1962) and it was recognized that the isothermal magnetization curve measures the thermodynamic magnetization only if it shows no hysteresis. Finnemore *et al* (1966) were the first to obtain reliable  $H_{c1}(T)$  for niobium by preparing samples to ensure no hysteresis in the isothermal magnetization curves.

The lower critical field in the high  $T_c$  materials was identified by various workers (see references quoted in Grover (1988); Chaddah (1988)) with the field value at which

the virgin ZFC magnetization deviates from the initial linear behaviour. Soon after the proliferation of magnetization data in these materials, we (Chaddah 1987; Grover *et al* 1988b) cautioned that the very large values of  $J_c$  in these materials result in gross overestimates of  $H_{c1}$ . The recent Bitter-patterns observed in  $\text{YBa}_2\text{Cu}_3\text{O}_7$  by Dolan *et al* (1989) confirm that flux pinning must be intrinsic to these superconductors, presumably because of their short coherence lengths. Since hysteresis free isothermal magnetization curves would thus not be possible in these materials, we had suggested a new criterion to estimate  $H_{c1}$  based on a low field anomaly in the hysteresis curve. The need for a new criterion appears to have been accepted (Yeshurun *et al* 1988; Hibbs *et al* 1988; Fruchter *et al* 1988; Krusin Elbaum *et al* 1989). Yeshurun *et al* suggested the use of magnetic relaxation rate to estimate  $H_{c1}$ . While the onset of relaxation should define  $H_{c1}$ , it was found to lack experimental accuracy. Yeshurun *et al* then incorporated  $H_{c1}$ , in a parametric way (not justified by them), into  $J_c(H)$  and obtained  $H_{c1}$  by fitting their relaxation data on YBCO. The same group (Krusin-Elbaum *et al* 1989) have proposed another criterion and claim to have determined the intrinsic  $H_{c1}$  in YBCO by analysing  $M_{\text{ZFC}}$  and  $M_{\text{rem}}$  data in a number of samples. Their analysis takes account of thermodynamic magnetization as well as shielding effects, including  $H_{c1}$  in a (different) parametric way. We shall first show that the values of  $H_{c1}$  obtained by the above two criteria are not consistent with both the sets (Krusin-Elbaum *et al* 1989; Malozemoff *et al* 1988a) of  $M_{\text{rem}}$ ,  $M_{\text{FC}}$  and  $M_{\text{ZFC}}$  data published by the same group.

As stated earlier, Malozemoff *et al* (1988a) have shown the validity of eq. (3) for  $H < H_{c1}$  (assuming  $N = 0$ ). We argued that the field at which relation (3) is replaced by relation (4) provides an upper limit to  $H_{c1}(T)$ . Figure 8 shows this to happen in a YBCO single crystal specimen of Malozemoff *et al* at  $T > 40\text{ K}$  for  $H = 60\text{ Oe}$ . Taking their quoted (see their table 2) demagnetization factor ( $N = 0.16$ ), this yields  $H_{c1}(\perp c)$  at  $40\text{ K}$  to be less than  $75\text{ Oe}$ . This is well below the corresponding value of about  $160\text{ Oe}$  given in figure 3 of Krusin-Elbaum *et al* (1989) and the  $H_{c1}(0)(\perp c) = 230\text{ Oe}$  quoted by Yeshurun *et al* (1988). In another crystal, for which only  $M_{\text{ZFC}}(T)$  and  $M_{\text{rem}}(T)$  data have been published (figures 1 and 2, Krusin-Elbaum *et al* 1989), it is easy to see that the equality would not be valid for  $H(\perp c) = 30\text{ Oe}$  at  $T > 50\text{ K}$ , and for  $H(\perp c) = 60\text{ Oe}$  at  $T > 20\text{ K}$ . The value of demagnetization factor for this crystal has not been explicitly given. However, from the range of values quoted for field applied along  $c$ -axis, it is easy to argue that for field perpendicular to  $c$ -axis,  $N$  would lie between  $0.05$  and  $0.25$ . Such a range for  $N$  would again imply  $H_{c1}(\perp c)$  to be less than  $80\text{ Oe}$  at  $25\text{ K}$ .

In our results on Nb rod sample, it is apparent that the transition from relation (3) to (4) occurs as  $H$  is increased from  $500\text{ Oe}$  to  $1000\text{ Oe}$ . Since our sample was not outgassed, it is expected to contain dissolved oxygen and/or nitrogen. Such samples of niobium were extensively studied by DeSorbo (1963, 1964), who found that  $T_c$  and  $H_{c2}$  varied with the extent of dissolved oxygen or nitrogen. The samples always show hysteresis, and one can thus record only the field at which flux penetration in the ZFC sample is first measurable. He found that flux penetration first occurs at  $H \sim 600\text{ Oe}$  for  $\text{Nb} + 0.124$  weight percent of oxygen. While we have not measured the oxygen (or nitrogen) content of our samples, we can state that the value of  $H_{c1}$  inferred for our Nb rod sample is not inconsistent with the existing data. For our Nb powder sample, relation (4) holds for  $H > 100\text{ Oe}$ , which we may identify with  $H_{c1}(1 - N)$ . Here  $N$  is the largest (and not the average value) demagnetization factor

amongst the arbitrary shaped and randomly oriented particles constituting our powder sample. We note that  $H_{c1}$  for powder sample could turn out to be smaller than that for the rod sample. This would appear consistent with the fact that the measured value of  $H_{c2}$  in Nb powder is about twice that in rod sample (Sarkissian *et al* 1989). DeSorbo (1963, 1964) had also found different  $H_{c2}$  values for niobium samples with different oxygen and/or nitrogen content. Our powder and rod sample may well be having different amounts of absorbed gases.

As pointed out earlier, 100 Oe is also the field value at which  $M_{FC}(H)$  shows a deviation from linearity (figure 1d) in Nb powder. It may be recalled that  $M_{FC}(H)$  is not complicated by contributions from macroscopic shielding currents. The value at which  $M_{FC}(H)$  deviates from linearity may thus provide a more reliable limiting value for  $H_{c1}(1 - N)$  in hard superconductors.

If we estimate  $H_{c1}$  values in YBCO, according to the above criterion, from the data of Malozemoff *et al* (1988a), they would turn out to be  $\sim 1$  Oe at 4.2 K. Such a low estimate for  $H_{c1}$  in YBCO need not be considered unrealistic. Lin *et al* (1988) have quoted  $H_{c1}(\perp c)$  to be 4.4 Oe at 7 K in single crystal specimen of high  $T_c$   $\text{Bi}_2\text{Sr}_2\text{CaCuO}_8$  ( $T_c = 85$  K) from the deviation of linearity of ZFC magnetization curve. The intragrain current densities in this family of superconductors are believed to be an order of magnitude smaller than in YBCO family, therefore the deviation from linearity of  $M_{ZFC}$  curve is expected to give a closer upper limit to its intrinsic  $H_{c1}$  value.

## 5. Conclusions

We have made various history dependent magnetization measurements in niobium samples. While the powder and rod samples show very different flux trapping on cooling in a field, we see strong similarities in the history effects on isothermal magnetization. All the features are qualitatively understood using our earlier ideas explaining history effects in high  $T_c$  superconductors. The observation of  $M_{rem}$  and the temperature dependence of  $(M_{rem} - M_{FC} + M_{ZFC})$  seen in high  $T_c$  superconductors are reproduced in a conventional hard type II superconductor. We identify clearly the existence of three field regions specifying the sign of  $(M_{rem} - M_{FC} + M_{ZFC})$ .

We show that the field at which the equality between  $(M_{rem} - M_{FC})$  and  $(-M_{ZFC})$  first breaks down provides a reasonable estimate of  $H_{c1}$  for the extensively documented case of niobium.

## Acknowledgements

We thank Dr B A Dasannacharya and Dr B V B Sarkissian for various discussions. We would also like to acknowledge Professors C Radhakrishnamurty, S S Jha and R Vijayaraghavan for their continuing interest in this work.

## References

Bean C P 1962 *Phys. Rev. Lett.* **8** 250  
 Bean C P 1964 *Rev. Mod. Phys.* **36** 31

Chaddah P 1987 *Proc. DAE Solid State Phys. Symp. A* **30** 95

Chaddah P 1988 *Prog. High Temp. Superconductivity* Vol. 16 (Singapore: World Scientific) 203; *Rev. Solid State Sci.* **2** 303

Chaddah P and Ravikumar G 1989 *Phase transitions* (in press)

Chaddah P, Ravikumar G, Grover A K, Radhakrishnamurty C and Subba Rao G V 1989 (submitted to *Cryogenics*)

DeSorbo W 1963 *Phys. Rev.* **123** 107

DeSorbo W 1964 *Phys. Rev.* **A134** 1119

Dolan G J, Chandrashekhar G V, Dinger T R, Feild C and Holtzberg F 1989 *Phys. Rev. Lett.* **62** 827

Finnemore D K, Stromberg T F and Swenson C A 1966 *Phys. Rev.* **149** 231

Fraser J R, Finlayson T R, Smith T F, Heintze G N, McPherson and Whitfield H J 1988 *Proc. of MRS Spring Meeting* (in press)

Fruchter C, Giovannella C, Collin G and Campbell I A 1988 *ORsay Preprints*, Supplement to Vol. 7—March 1988

Grover A K 1988 *Prog. High Temp. Superconductivity* Vol. 16 (Singapore: World Scientific) 211; *Rev. Solid State Sci.* **2** 311

Grover A K, Radhakrishnamurty C, Chaddah P, Ravikumar G and Subba Rao G V 1988a *Pramāṇa—J. Phys.* **30** 569

Grover A K, Radhakrishnamurty C, Chaddah P, Ravikumar G and Subba Rao G V 1988b *Pramāṇa—J. Phys.* **30** L167

Hauser J J 1962 *Phys. Rev. Lett.* **9** 423

Hibbs A D, Eberhardt F J, Campbell A M and Male S 1988 *Cryogenics* **28** 678

Krusin-Elbaum L, Malozemoff A P, Yeshurun Y, Cronemeyer D C and Holtzberg F 1989 *Phys. Rev. B* **39** 2936

Lewis R T 1971 *Rev. Sci. Inst.* **42** 31

Malozemoff A P, Krusin-Elbaum L, Cronemeyer D C, Yeshurun Y and Holtzberg F 1988a *Phys. Rev. B* **38** 6490

Malozemoff A P, Yeshurun Y, Krusin-Elbaum L, Worthington T K, Cronemeyer D C, Dinger T, Holtzberg F and McGuire T R 1988b, *Proc. Latin-American Conference on High Temperature Superconductivity, Prog. High Temp. Superconductivity* (Singapore: World Scientific) Vol. 19

Lin J J, Benitez E L, Poon S J, Subramanian M A and Sleight A W 1988 *Phys. Rev. B* **38** 5095

Müller J and Olsen J L (eds) 1988 *Proc. Int. Conf. High Temp. Superconductors and Materials and Mechanisms of Superconductivity* (Amsterdam: North Holland); reproduced as *Physica* **C153–155**

Müller K A, Takashige M and Bednorz J G 1987 *Phys. Rev. Lett.* **58** 1143

Ravi Kumar G and Chaddah P 1988 *Pramāṇa—J. Phys.* **31** L141

Rossel C, Maeno Y and Morgenstern I 1989 *Phys. Rev. Lett.* **62** 681

Sarkissian B V B, Grover A K, Balakrishnan G, Paulose P L and Vijayaraghavan R 1989 *Physica C* (to be published)

Schiedt E W, Schaefer M, Riesemeier H and Luders K 1988 *Physica C153–155* 391

Yeshurun Y and Malozemoff A P 1988 *Phys. Rev. Lett.* **60** 2202

Yeshurun Y, Malozemoff A P, Holtzberg F and Dinger T R 1988 *Phys. Rev. B* **38** 11828

#### Note added in proof

After the acceptance of this paper, we have come across new results on  $M_{FC}(H \perp c)$  in two YBCO single crystals showing different extents of flux trapping on field cooling (see data of D C Cronemeyer and F Holtzberg in figure 2 of A P Malozemoff in 'Physical Properties of High Temperature Superconductors I', ed. D M Ginsberg, World Scientific, Singapore, 1989—Progress in High Temperature Superconductivity Vol. 7).  $M_{FC}(H)$  data show deviation from linearity at  $H = 10$  Oe in both these samples. The data are reported to be at low temperature, and for the stated values of the thickness of the samples, demagnetization factor will be negligible. These would imply  $H_{c1}(H \perp c)$  to be  $\sim 10$  Oe in YBCO, as per the new criterion suggested in this paper.